Hindawi Publishing Corporation
Journal of Computational Engineering
Volume 2014, Article ID 310358, 15 pages
http://dx.doi.org/10.1155/2014/310358

Research Article

Effects of Lateral Window Position and Wind Direction on Wind-Driven Natural Cross Ventilation of a Building: A Computational Approach

M. Z. I. Bangalee,[1] J. J. Miau,[2] S. Y. Lin,[2] and M. Ferdows[1]

[1] *Department of Mathematics, University of Dhaka, Dhaka 1000, Bangladesh*
[2] *Department of Aeronautics and Astronautics, National Cheng Kung University, Tainan City 701, Taiwan*

Correspondence should be addressed to M. Z. I. Bangalee; raaz2015@yahoo.com

Received 18 November 2013; Revised 21 January 2014; Accepted 30 January 2014; Published 11 March 2014

Academic Editor: Clement Kleinstreuer

Energy is saved when an effective natural ventilation system can provide comfort air to the occupants in a building by replacing a mechanical ventilation system. It also minimizes the risk of the environmental pollution and the global warming. A one story, full scale building was considered to carry out a comparative study of three different cases of wind-driven natural (WDN) cross ventilation with the help of computational fluid dynamics (CFD). In each case, the location of window was changed in lateral direction to predict the probable position for optimum ventilation performance and the angle of wind was varied to check the sensitivity of the wind direction on the flow field. After validating the current methodology through two satisfactory comparisons with the experimental investigations, the governing equations subjected to the corresponding boundary conditions were solved using commercial software and then the results were analyzed. A better location for the windows in each case was proposed. The ventilation purpose was served quite well even if the wind angle was changed in a moderate range from the original design. Furthermore, the velocity components, ventilation rate, surface pressure, ventilation time, and so forth in each case were investigated and compared extensively with those in other cases.

1. Introduction

Ventilation is a system in which the internal air is continuously replaced from an occupied space by the relatively fresh outside air through vents, windows, doors, and so forth. There are several reasons such as warm temperature, odors, smokes, pollutions, humidity, suffocation, and so forth which may often disrupt the occupant's physical comfort. Three types of ventilation system are available such as forced ventilation, natural ventilation, and hybrid ventilation to improve the indoor air quality. Forced ventilation is served by powering a mechanical system such as fans, blowers, and so forth to push the external air into the space of interest. It is needless to note that this ventilation system consumes electric power in operation. On the other hand, natural ventilation system neither consumes electric power nor needs any mechanical system. It is the system where the flow is induced naturally by the temperature and/or pressure differences between spaces. If the mechanical and the natural components are introduced in conjunction to ventilate the desired space, then it is known as hybrid ventilation system. It is useful when the natural ventilation cannot serve the purpose completely due to unexpected weather conditions.

In buildings, electric power is mostly consumed by heating, ventilation, and air-conditioning (HVAC) systems. According to Awbi [1] ventilation consumes 30–60% of the total energy consumption in modern and retrofit buildings. The fossil fuel and nuclear power based electricity generations are discouraged by the modern science and the fact due to the global warning, the environmental pollution, and the safety matter. In addition to this, an attempt to enhance the green energy generation is expected to be observed all over the globe to meet the growing energy demand. As the green energy with its present technology and efficiency is

not able to meet the entire energy demand, a reduction of energy consumption is desired. Fordham [2] studied the natural ventilation case extensively and concluded that buildings were needed to be designed with natural ventilation in mind to minimize the use of fossil fuel energy. Since natural ventilation system does not require any mechanical component or electric power to provide the fresh air, it is an energy saving system. Besides, if the external environment and condition permit, it can also be used to replace the internal air from a building in remote and desert areas where the electric power is not available.

A plenty of research on natural ventilation was carried out in the last four decades. Cockroft and Robertson [3] investigated the ventilation of an enclosure through a single opening and derived a simple theoretical model to predict the airflow by measuring the wind-driven ventilation subjected to impinging air stream. Cermak et al. [4] reviewed the requirements for similarity of natural ventilation in wind tunnel models and experimental methods for evaluating its effectiveness. Based on the design and position of the opening, a natural ventilation system can be divided into two categories such as the cross ventilation [5] and the single-sided ventilation [6]. Air is naturally driven in/out of the building due to the pressure and/or the temperature differences across the openings which result from the wind-driven force and/or the buoyancy-driven force. A number of investigations were reported to study the performance of the wind-driven ventilation [7], buoyancy-driven ventilation [8], or the combination of wind-driven and buoyancy-driven ventilation [9].

The experimental observation [10] and the numerical computation [11] are common approaches to investigate the physics of WDN ventilation as well as buoyancy-driven natural ventilation. In addition to these, combination of experimental and numerical investigation is also common in this field as done by Jiang et al. [12]. Recently, CFD has attracted huge attention because it may provide an accurate alternative to scale model testing, with variations on the simulation being performed quickly. The continuous development of the computer speed and the turbulence modeling encourage the researchers to adopt CFD to investigate any problem associated with fluid dynamics and heat transfer. In particular, a number of relevant CFD investigations in natural ventilation were reported in the last few years. A few among many can be found in [13–18]. For brevity, only the most relevant references have been discussed in the corresponding sections. However, the proper application of CFD in wind engineering field is always challenging and some guidelines [19] should be followed to minimize the inaccuracy.

In most cross ventilation studies, openings/windows are located face to face. However, some cross ventilated buildings may not have the windows be located face to face due to some specific reasons. In addition, the investigations of the ventilation through a single opening (on a specific wall) may not exactly predict the airflow through multiple windows. Therefore, the investigations of WDN ventilation through face to face windows (one on the front wall and the other on the rear wall), diagonal windows (one on the front wall and the other on the rear wall), and multiple windows (two on the front wall and two on the rear wall) of a full scale, one story building were accomplished and compared in the present study. Furthermore, the effects of the window locations and the wind angles were also investigated to locate the optimum window location and to check the wind direction sensitivity on the flow field, respectively. To the authors' knowledge, no study has been reported where a comparative study of cross ventilation through multiple windows and diagonally positioned windows was carried out varying the window location and the wind angle.

Three different cross ventilation cases based on the number and location of windows were investigated with the help of CFD. For each case, the window locations and wind angles were varied, analyzed, and compared with other cases. A nonuniform fully structured gird and Renormalization-Group of turbulence (RNG) k-ε [20] model were chosen as the grid type and turbulence model, respectively, which have been described in the relevant sections of this paper in detail. The Reynolds averaged Navier-Stokes equations together with the proper boundary conditions were solved with the software, ANSYS CFX [21] and then the results were analyzed.

2. The Investigated Model

WDN cross ventilation through square shaped windows was considered to investigate the flow phenomena inside and around a full scale building of wall thickness 0.25 m. The detailed description of the computational domain, the building, and the windows were shown in Figure 1. The porosity ($100 \times A_{\text{window}}/A_{\text{wall}}$) induced by each window was 3.33%. The reason of choosing the present domain size has been clarified in Section 3.2. The maximum distance between the center of the window and the centerline of the building (DWC) was 1.475 m (Figure 1(b)). This distance was varied to investigate the effect of the location of the window on the WDN cross ventilation. The distance, DWC was nondimensionalized by dividing it with the half wall length (i.e., NDDW = DWC/2 m). Two windows on the same wall (or diagonally positioned on different walls) were symmetrical about the streamwise centerline of the building.

The name of the walls and windows and the window locations were indicated in Figure 2. The angle between the approaching wind direction and the length (along Y axis) of the building was termed as wind angle, α which was varied to investigate the wind direction effect on the present WDN cross ventilation system. Depending on the number and the location of windows, the following cross ventilation cases were considered:

Case 1: face to face cross ventilation through four openings;

Case 2: face to face cross ventilation through two openings;

Case 3: diagonal cross ventilation through two openings.

All four windows (window 1–window 4) were opened in Case 1, whereas window 1 and window 4 in Case 2 and window 1 and window 3 in Case 3 were opened. To analyze

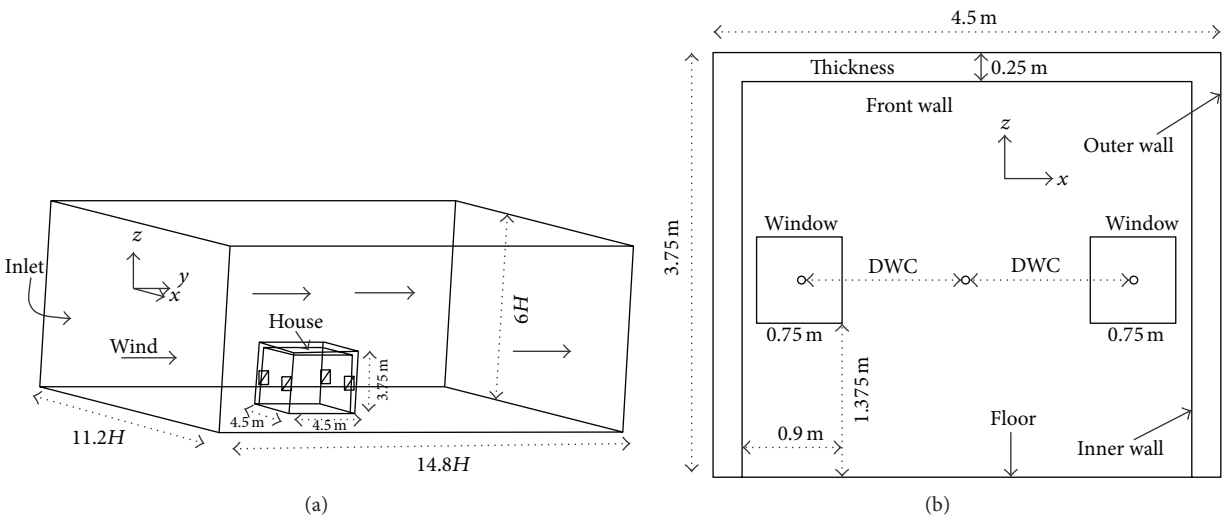

Figure 1: The schematic view, positions, and dimensions of (a) the computational domain and (b) the windows on the front wall.

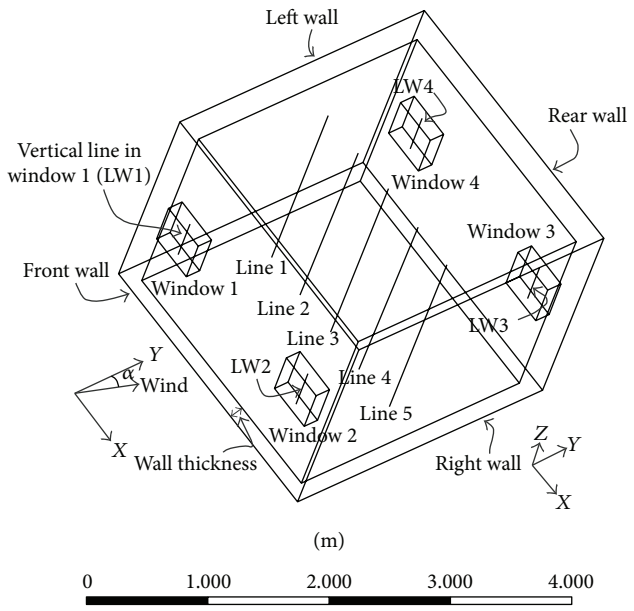

Figure 2: The schematic view of the building and the locations of calculation.

the flow phenomena inside the building, five vertical lines (line 1–line 5 in Figure 2), which were equidistant from the front and the rear wall, were chosen as the locations of calculations.

3. Numerical Methodology

The numerical solution of the present system was obtained by following several systematic steps corresponding to CFD. The success of any particular numerical approach predominantly depends on the precision of the following steps.

3.1. Flow Characteristics and Grid Generation. The fluid was air (i.e., Newtonian) having constant property. The flow was assumed steady, three-dimensional, viscous, turbulent, incompressible, and isothermal. A nonuniform structured mesh with stretching factor 1.1–1.3 was generated using the software ICEM CFD [21] to discretize the computational domain. The finest possible grid distribution was used that contained approximately 1.8-1.9 million hexahedral elements (circled in Figure 3). Relatively smaller elements were introduced inside the building. The smallest spacing of the grid was 1-2 mm and was set to the near wall (inside and outside of the building) to capture the boundary effect on the flow field properly. The grid near the wall was generated in such a way that a sufficient number of grid points were within the boundary layer thickness (δ) that was estimated from the turbulence boundary layer thickness along a flat plate $\delta = 0.16L/\mathrm{Re}^{1/7}$ [22]. The grid independence tests were carried out utilizing meshes with up to 3.92 million elements and the results reveal that the discrepancy in the ventilation rate through the inlet was below 1.7% (Figure 3). Hence, it can be stated that the present grid system was adequate to capture the flow characteristics with an acceptable accuracy.

3.2. Computational Domain and Turbulence Model. Hargreaves and Wright [23] suggested that if the unmodified commercial code was used, then as short a fetch as possible was in fact more desirable. However, Tominaga et al. [24] provided the specific guidelines regarding the computational domain size for practical applications of CFD to pedestrian wind environment around buildings in atmospheric boundary layer. The computational domain in the present study was ensured to be large enough under the guideline of [23, 24]. A sensitivity analysis was carried out to check the domain size effect on the present ventilation system. The velocity distribution on a line from the front window to the rear window (when the windows were located at the mid of the

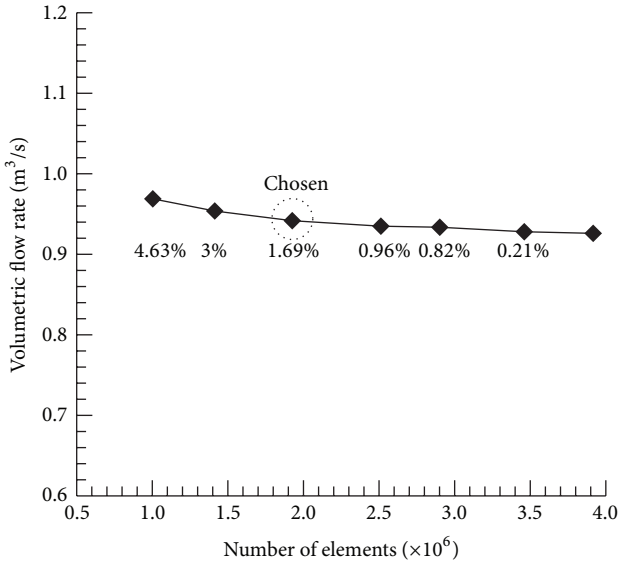

FIGURE 3: Volumetric flow rate through inlet in Case 1 for different grid distribution.

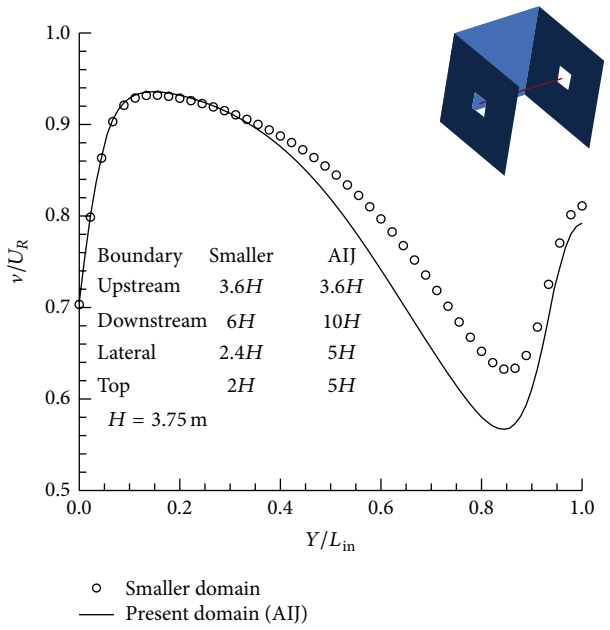

FIGURE 4: Indoor velocity distributions obtained from two computational domains.

corresponding walls) in Case 2 was shown and compared in Figure 4. Although, the results obtained from a reduced domain size and AIJ's (Architectural institute of Japan) recommended domain size [24] showed negligible difference in ventilation rate (below 0.32%), a larger quantitative flow difference (maximum 12% in Figure 4) was observed inside the building. The inlet, lateral, top, and outlet boundary of the present computational domain were 3.6 H, 5 H, 5 H, and 10 H away from the building. The blockage ratio was 1.79%.

The flow around a building (bluff body) is fully turbulent when $\mathrm{Re}_b > 2 \times 10^4$, whereas the flow of air discharging through a window (opening) would become turbulent when $\mathrm{Re}_w > 300$ [4]. Therefore, the flows inside and around the building are turbulent unless the velocities are below the critical values. As $\mathrm{Re}_b \gg 2 \times 10^4$ and $\mathrm{Re}_w \gg 300$, the flow was fully turbulent in the present study. Several numerical models are available and commonly used to predict the turbulence in natural ventilation system. Among the available models, large-eddy simulation (LES) [25] and Reynolds averaged Navier-Stokes equations were frequently used. A more detailed literature survey regarding the application of various turbulence models in predicting naturally ventilated flow can be found in [13, 16, 18]. Chen [26] investigated eight different turbulence models to study indoor airflows and concluded that RNG k-ε model might be the best. Furthermore, the present study has also found this turbulence model capable to capture the internal flow in acceptable order of accuracy which has been proved to be valid through two comparisons in Section 3.4. Therefore, RANS with RNG k-ε turbulence model was chosen to predict the flow field in the present WDN cross ventilation systems.

3.3. Governing Equations and Boundary Conditions. According to the flow characteristics, the RANS equations for a Newtonian fluid are given by

continuity:

$$\frac{\partial}{\partial x_j}\left(U_j\right) = 0; \quad j = 1, 2, 3 \tag{1}$$

momentum:

$$\rho U_j \frac{\partial}{\partial x_j}\left(U_i\right) = -\frac{\partial p}{\partial x_i} + \frac{\partial}{\partial x_j}\left[\left(\mu + \mu_T\right)\frac{\partial U_i}{\partial x_j}\right]; \quad i = 1, 2, 3, \quad j = 1, 2, 3. \tag{2}$$

It is assumed that the turbulence viscosity, (μ_T) is related to the turbulence kinetic energy (k) and dissipation rate (ε) as

$$\mu_T = C_\mu \rho \frac{k^2}{\varepsilon}. \tag{3}$$

The transport equations for k and ε are

$$\rho \frac{\partial}{\partial x_j}\left(U_j k\right) = \frac{\partial}{\partial x_j}\left[\left(\mu + \frac{\mu_T}{\sigma_k}\right)\frac{\partial k}{\partial x_j}\right] + P_k - \rho\varepsilon,$$

$$\rho \frac{\partial}{\partial x_j}\left(U_j \varepsilon\right) = \frac{\partial}{\partial x_j}\left[\left(\mu + \frac{\mu_T}{\sigma_\varepsilon}\right)\frac{\partial \varepsilon}{\partial x_j}\right] + \frac{\varepsilon}{k}\left(C_{\varepsilon 1} P_k - C_{\varepsilon 2}\rho\varepsilon\right), \tag{4}$$

where

$$P_k = \mu_T\left(\frac{\partial U_i}{\partial x_j} + \frac{\partial U_j}{\partial x_i}\right)\frac{\partial U_i}{\partial x_j}; \quad i = 1, 2, 3, \quad j = 1, 2, 3. \tag{5}$$

In the above equations C_μ, $C_{\varepsilon 1}$, $C_{\varepsilon 2}$, σ_k, and σ_ε are constants. The values of these constants are empirical which differentiate

Table 1: Constants used in the turbulence models.

Symbols of constants	k-ε	RNG k-ε
C_μ	0.09	0.085
$C_{\varepsilon 1}$	1.44	$1.42 - \dfrac{\eta(4.38-\eta)}{4.38(1+\beta\eta^3)}$
$C_{\varepsilon 2}$	1.92	1.68
σ_k	1.0	0.7179
σ_ε	1.3	0.7179
η	—	$\sqrt{\dfrac{P_k}{\rho C_{\mu\text{RNG}}\varepsilon}}$
β	—	0.012

between k-ε and RNG k-ε turbulence model. RNG k-ε turbulence model is expected to predict the larger dissipation rate in laminar regions near solid surface more accurately. The values of the empirical constants used in the both turbulence models have been shown in Table 1.

The boundary conditions along with the locations are as follows:

(1) velocity inlet: upstream boundary (U_R = 1.5 m/s);

(2) zero static pressure (opening): top, rear, and lateral (side) boundaries of the computational domain around the building;

(3) no slip wall: ground of the surrounding and all surfaces of the building.

3.4. Numerical Solution and Comparisons. The converged, grid independent, and minimum fourth-order accurate numerical solution of the WDN cross ventilation through multiple windows was obtained by using the software ANSYS CFX [21] to solve the governing equations along with the boundary conditions at each grid of the computational domain. The convergence history of the fifth-order residual target for the flow components and turbulence quantities are presented in Figure 5 when Case 2 having window at the mid wall is considered. The present methodology was validated through comparisons with two experimental works.

3.4.1. Comparison 1. Karava et al. [5] reported the experimental study of wind-driven cross-ventilation flow based on Particle Image Velocimetry (PIV) method in a boundary layer wind tunnel. The 2 mm thick reduced scale model was 10 cm (W) × 8 cm (H) × 10 cm (D) and was tested with different window arrangements. Among the total nine experimental cases (A1, A2, B1, B2, C1, C2, D1, D2, and E1), one case (case E1) with porosity 5% and 10%, which was more close to the present study was solved numerically in order to justify the methodology. The readers are referred to Karava [27] for more information about the original experimental work. AIJ's recommendations [24] and the upstream length 3 H were considered to build the computational domain around the model. The following inlet boundary conditions proposed by Tominaga et al. [24], Karava [27], and Ramponi,

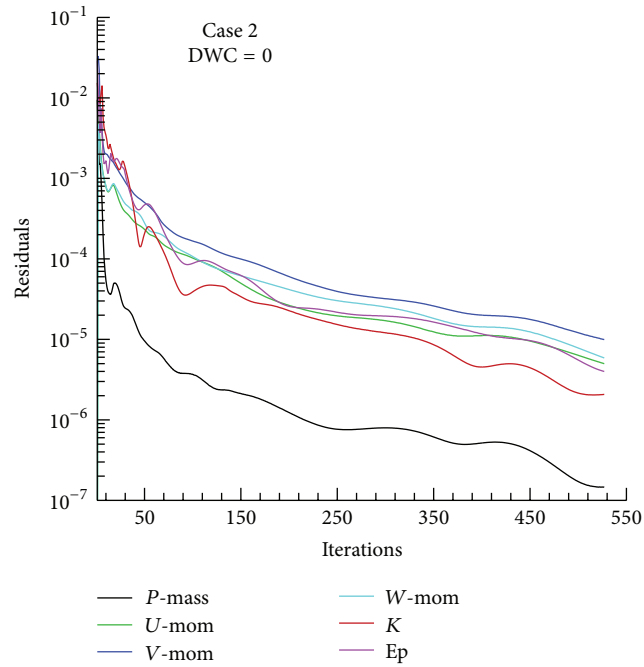

Figure 5: Convergence of Case 2.

and Blocken [18] were found satisfactory which were applied to predict the internal and external flow conditions:

$$v^* = \frac{0.42 v_h}{\ln\left(\left(H + z_0\right)/z_0\right)},$$

$$I(z) = \frac{1}{\ln\left(z/z_0\right)},$$

$$v(z) = \frac{v^*}{0.42} \cdot \ln\left(\frac{z + z_0}{z_0}\right), \tag{6}$$

$$k(z) = \left(I(z)\, v(z)\right)^2,$$

$$\varepsilon(z) = \frac{v^{*3}}{0.42\left(z + z_0\right)}.$$

Symmetry conditions were set to the lateral and the top boundaries of the computational domain, whereas the downstream boundary was set as opening with zero relative pressure. A sum of 945218 hexahedral elements was generated in the computational domain with stretching factor 1.2 and minimum size 0.5 mm. The minimum residual target 10^{-4} for momentum and continuity was achieved in all cases. Figures 6(a) and 6(b) show the nondimensionalized velocity in the downstream direction on a line through inlet and outlet for porosity 5% and 10%. The simulations with SST and RNG k-ε turbulence model predicted the flow more accurately than that with k-ε and k-ω turbulence models. However, the oscillatory convergence behaviour was observed only in SST model's flow prediction, whereas other three models showed smooth convergence in 10% porosity case. It is notable here that the convergence target 10^{-6} in RNG k-ε turbulence model's flow prediction was achieved by 200 iterations only.

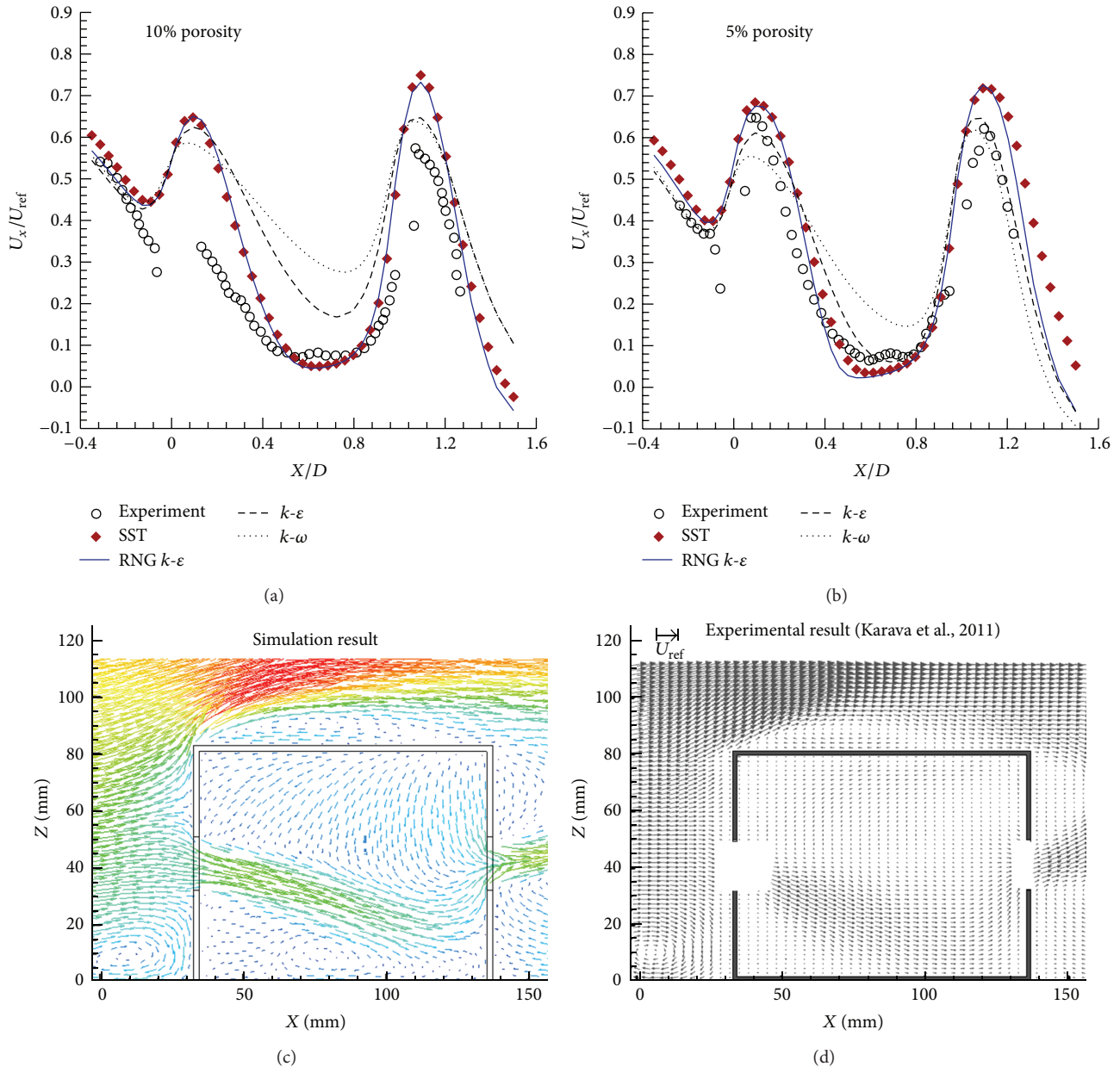

FIGURE 6: Comparisons between experimental [5] and simulation results.

Though SST model predicted the experimental results slightly better, this study chose RNG k-ε model that provided the converged results one order of magnitude faster than SST turbulence model did. The computational velocity vector field (Figure 6(c)) on a vertical center plane was compared with that of the experiment (Figure 6(d)) and was found satisfactory. A similar comparative result was reported by Ramponi and Blocken [18]. A larger disagreement was observed in the vicinity of the inlet and outlet and can be attributed to the reflections and shading effects during the PIV experiments [5, 18]. Therefore, the present simulation approach with RNG k-ε turbulence model was able to predict the internal and external velocity vector, flow swirling, and flow quantity well.

3.4.2. Comparison 2. Cross ventilation through two door-like identical openings (84 mm × 125 mm) of a building-like cube (each side, H = 250 mm) with wall thickness 6 mm was simulated and compared with the original experimental results reported by Jiang et al. [12]. A grid independent and nonuniform structured mesh of 0.86 million elements with stretching factor 1.2 and 1 mm initial height near the wall was used. Jiang et al. [12] showed the velocity components on some vertical lines (each comprising of 18 points) at the center section of the model. The suitable boundary conditions of the computational domain for predicting this wind tunnel results can be found in Evola and Popov [13] and Richards and Hoxey [28]. The comparisons between the simulation velocity

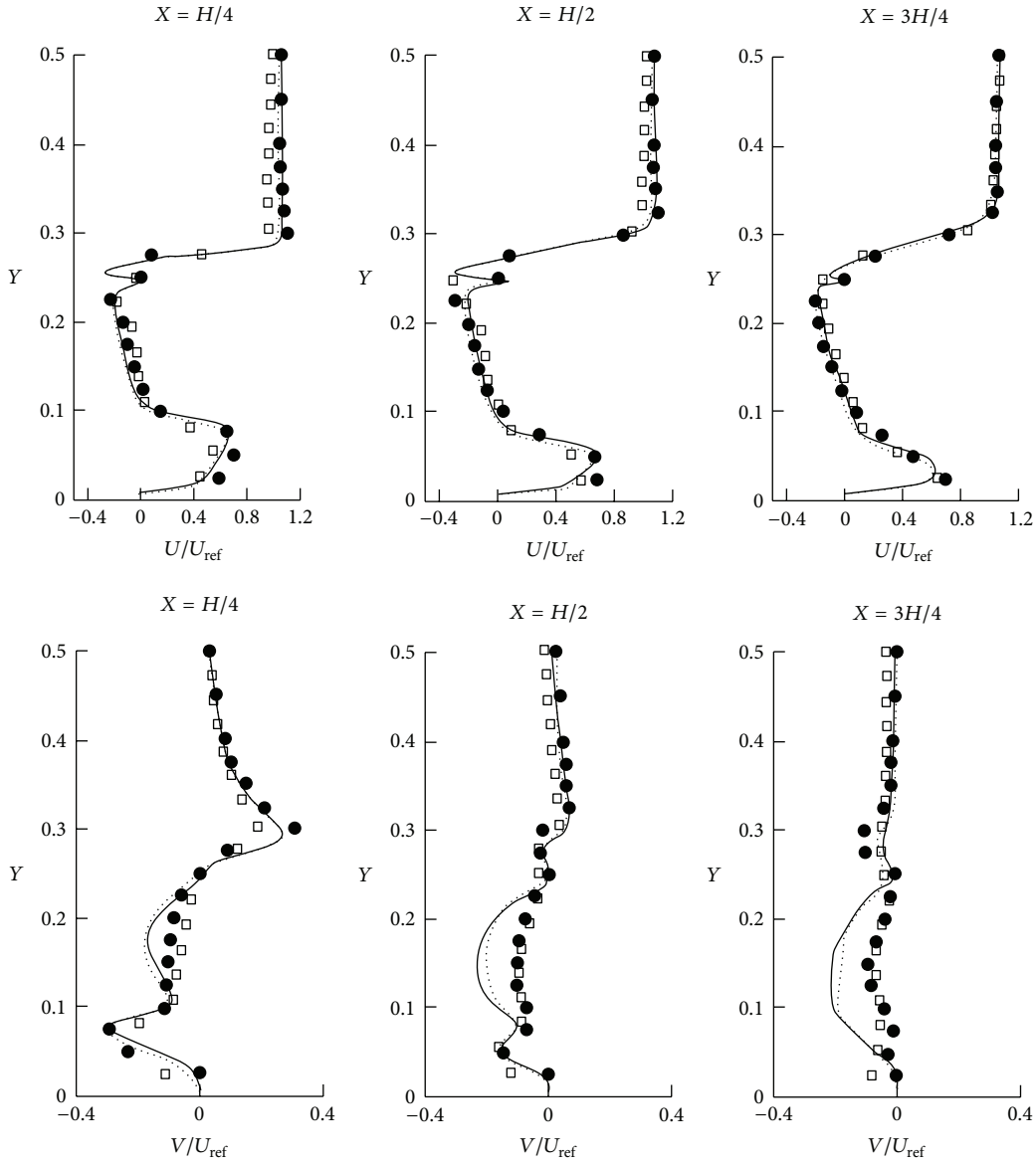

Figure 7: Comparison of mean velocity distributions between the values obtained from the present simulation approach and the experiment [12] for the cross ventilation. Square: present; black circles: experiment [12]; other lines: LES [12].

components and the experimental velocity components were depicted in Figure 7. The simulation results were found in good agreement with the experimental results of cross ventilation.

4. Results and Discussion

An effective ventilation system is that which replaces the internal air at its maximum extent. Therefore, it is obvious that the mass flow rate ($\dot{m} = \rho A v_w$) or the volumetric flow rate ($Q = A v_w$) through the inlet/outlet is the most important parameter for the evaluation of any ventilation system. However, it is customary to represent the ventilation rate by the volumetric flow rate. For simple experimental cases, a semiempirical relation, $Q = C_d A\sqrt{2\Delta p/\rho}$, is often used to calculate the WDN ventilation rate if the pressure difference across the openings is known. But this empirical relation is very sensitive to the value of C_d and the locations of measuring Δp. Dascalaki et al. [6] stated that for large external openings, where the impact of the wind on the air flow was not negligible, there were no appropriate methodologies to calculate the values of C_d and this introduced an important source of uncertainty. Moreover, this empirical relation does not take the ventilation type, window location, and wind direction into account. However, Table 2 represents some values of C_d that were considered to study natural ventilation systems recently. Using the above empirical relation, Δp was calculated here from the inlet and outlet pressure to predict the discharge coefficient. As is shown in Table 2, C_d is in the range of 0.61~0.98 for all window locations and wind

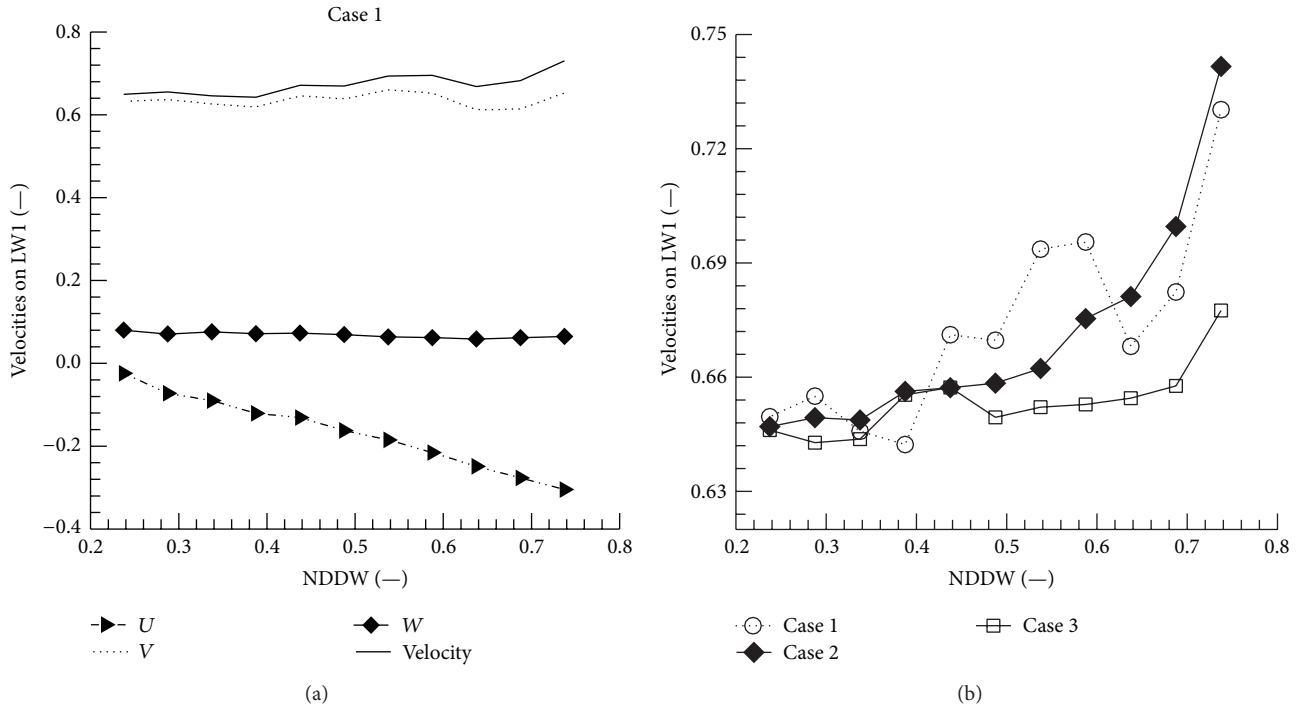

Figure 8: Velocities on LW1 at different window locations.

Table 2: Values of C_d.

Literatures	C_d
Dascalaki et al. [6]	0.6~1.0
Carey and Etheridge [10]	0.65~0.77
Jiang et al. [12]	0.78
Evola and Popov [13]	0.61
Present	0.61~0.98

directions in the present three cases. If the flow reaches its steady condition, the window located in the windward wall serves as inlet, whereas the window on the leeward wall serves as outlet in the cross ventilation system. As the mass is conserved, the volumetric flow rate through the inlet and the outlet is equivalent in magnitude. In the present study, the ventilation rate ($Q = \dot{m}/\rho$) is calculated directly from the mass flow rate entering the building through the inlet (or leaving through outlet).

Figure 8 shows the distribution of the nondimensional velocity components on line LW1 at different window locations (when $\alpha = 0^\circ$, $U_R = 1.5$ m/s) in Case 1. It is needless to mention that the velocity component V dominates the flow field at the window as well as in the outdoor flow field. The magnitudes of the velocity components U and W strengthen as the two windows move far from each other (Figure 8(a)). The behavior of the velocity components and thus the velocity are similar in all three cases. It is found (Figure 8(b)) that the resultant velocity (also V component) shows somewhat random decreasing-increasing trends as the distance between two windows increases in Cases 1 and 3. But in Case 2, it shows the increasing trend. Among all three cases, the magnitude of the velocity (also V component) is slightly smaller in Case 3 (Figure 8(b)) because there is no face to face window arrangement in this case and thus the entered fluid must travel the lateral distance from inlet to outlet before it exits through the outlet that produces more friction forces to be balanced. If the windows are located nearly mid of the corresponding wall (i.e., NDDW < 0.3), the velocity in Case 1 is the largest in all cases. However, at this moment we cannot conclude that this local phenomenon may ensure the highest ventilation rate because there are other important considerations to be accounted. Furthermore, if the windows are located near to the side wall (NDDW > 0.65), the velocity at this window in Case 2 shows the highest value in all cases (Figure 8(b)).

To have an insight of the internal flow dependence on the position of windows, five vertical lines (line 1–line 5) are introduced in Section 2. All these lines are fixed and equidistant from the front and the rear wall. In addition to this, line 3 is equidistant from the left and the right wall; that is, it is located at the mid of the building. Line 1 and line 2 are symmetrical to line 5 and line 4 (with respect to line 3), respectively. In Case 1, the regions around line 1 and line 5 are mostly dominated by the entering fluid through the left and the right windows, respectively, and thus the velocity distributions on them are nearly symmetric (Figure 9(a)). But these symmetric flow characteristics are not observed on lines 2 and 4 that may be attributed to the unsteady behavior of the mixing of the coming streams through different windows. No symmetric flow behavior is observed in Case 2 (Figure 9(b)) and Case 3 (Figure 9(c)) due to the asymmetric boundary conditions. In the latter two cases, line 1 and line 2 are no

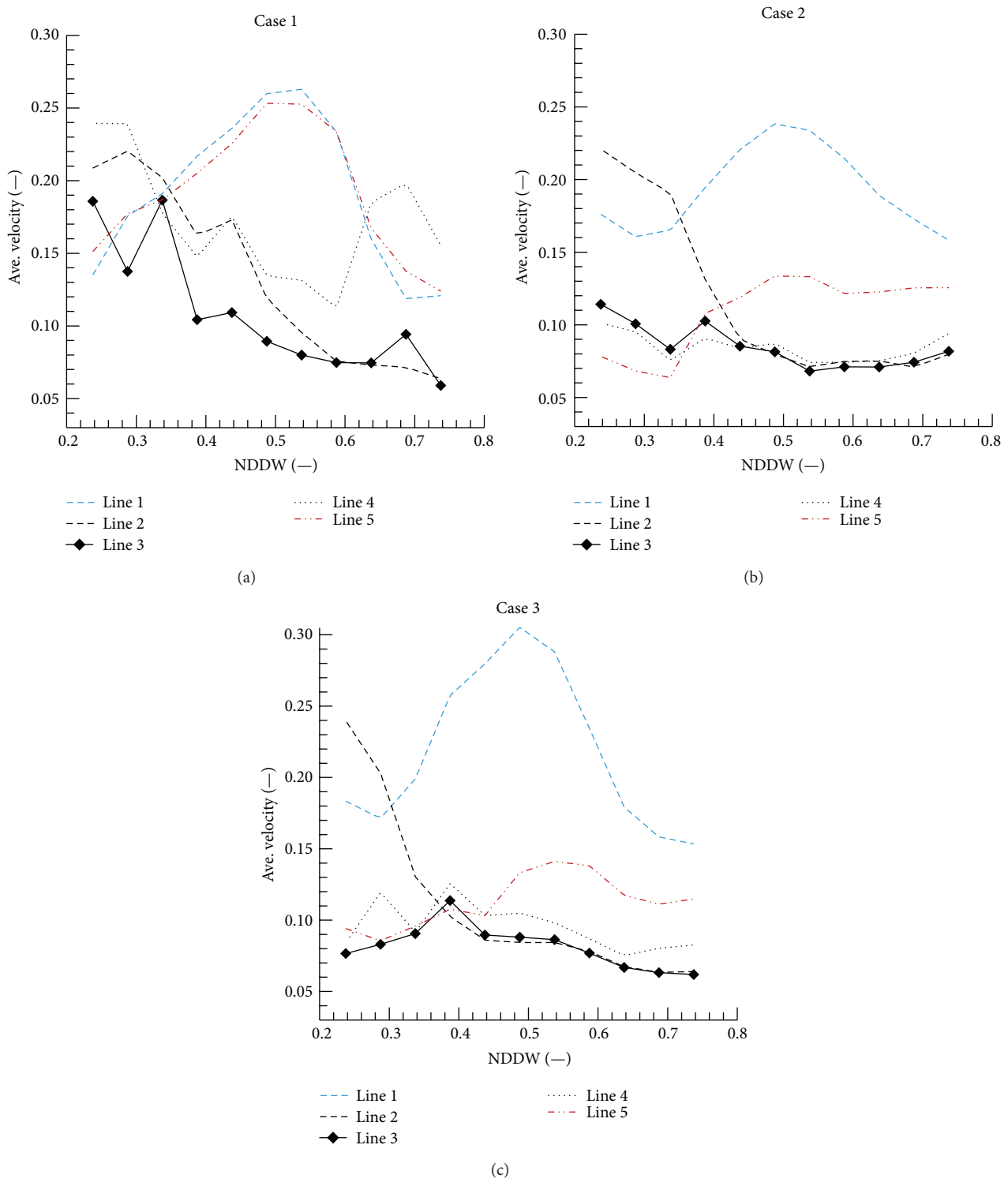

FIGURE 9: Average velocity on different lines inside the building.

more symmetrical (with respect to inlet and/or outlet) to line 5 and line 4, respectively. In all cases, the velocity on the five lines changes randomly with the change of window location. No regular or remarkable change is observed if the location of the window is changed. Nevertheless, the range of the velocity on these lines is 0.075 m/s–0.47 m/s when the free stream velocity is 1.5 m/s. The random change of the velocity with the change of NDDW inside the building establishes that the internal flow is influenced by the locations of the windows. The internal average velocity in Case 1 is slightly

higher (Figure 9(a)) than those in other cases (Figures 9(b) and 9(c)). The similar changing trend of the velocity with respect to NDDW in different cases on some lines indicates that the flows in different window locations experience the similar interactions, for example, velocity on line 1 in all cases. If a particular indoor location is aimed to have any specific flow range, Figure 9 may help the designers to guess the probable location of the windows.

Two identical windows are opened in Cases 2 and 3 whereas four windows are opened in Case 1. Therefore, at steady condition the volumetric flow rate Q through the inlet in Case 1 is much larger (and thus t is less) than those in Cases 2 and 3. As one of the main objectives of this research is to determine the position of windows for optimum ventilation, it is worthwhile to analyze and compare the nondimensional volumetric flow rate through the inlet/outlet at different window locations for all cases in detail. The nondimensional ventilation rate (Q/Q_{ref}) at different window locations is shown in Figure 10(a), whereas the required time, $t \propto 1/Q$, at each window location to replace the whole internal air can be obtained in Figure 10(b). In Case 1, it is found that if the windows are located as close as possible, the ventilation performance is increased and thus the required time for replacing the internal air is reduced. That is, if the windows are located in the central area of the windward and the leeward wall, it may provide more ventilated air (in shorter time). Therefore, it can be stated that one window in the central area of the front/rear wall can provide comfort air faster than those through two split windows located at two corners of the front and the rear walls. The overall ventilation performance is dependent on the window position by approximately 20%. However, the change of the ventilation performance with respect to the window position is found nonregular in Case 1. It is to be noted here that the steady mass flow rate is obtained from the balance of the wind force with the friction force. By its own nature, the indoor flow is more complex and chaotic in Case 1 than the flows in other cases. The dependence of ventilation performance on the position of multiple windows (Case 1) can be rechecked with the state of the art unsteady simulations or with experimental investigations based on Particle Image Velocimetry (PIV) method. As no such research is reported so far as well as it is also beyond the scope of the present study, the results reported here can be regarded as the first step prediction based on the standard steady state numerical approach.

The ventilation rate in Case 2 is stronger if the windows are located at the mid wall as well as in the corner area (Figure 10(a)). It is lower around NDDW ≈ 0.6. In Case 3, the ventilation rate depends on the lateral position of windows linearly. The more the windows are close to each other, the higher the ventilation rate. However, the volumetric flow rate through the inlet/outlet in Case 3 is found relatively small comparing to the performance of Cases 1 and 2. As there is no face to face window arrangement in this case, the whole entered air particles experience more interaction and collision and finally get its way to exit through the window located on the rear wall. Although the ventilation time in Case 3 is higher than that of other cases (Figure 10(b)), it may

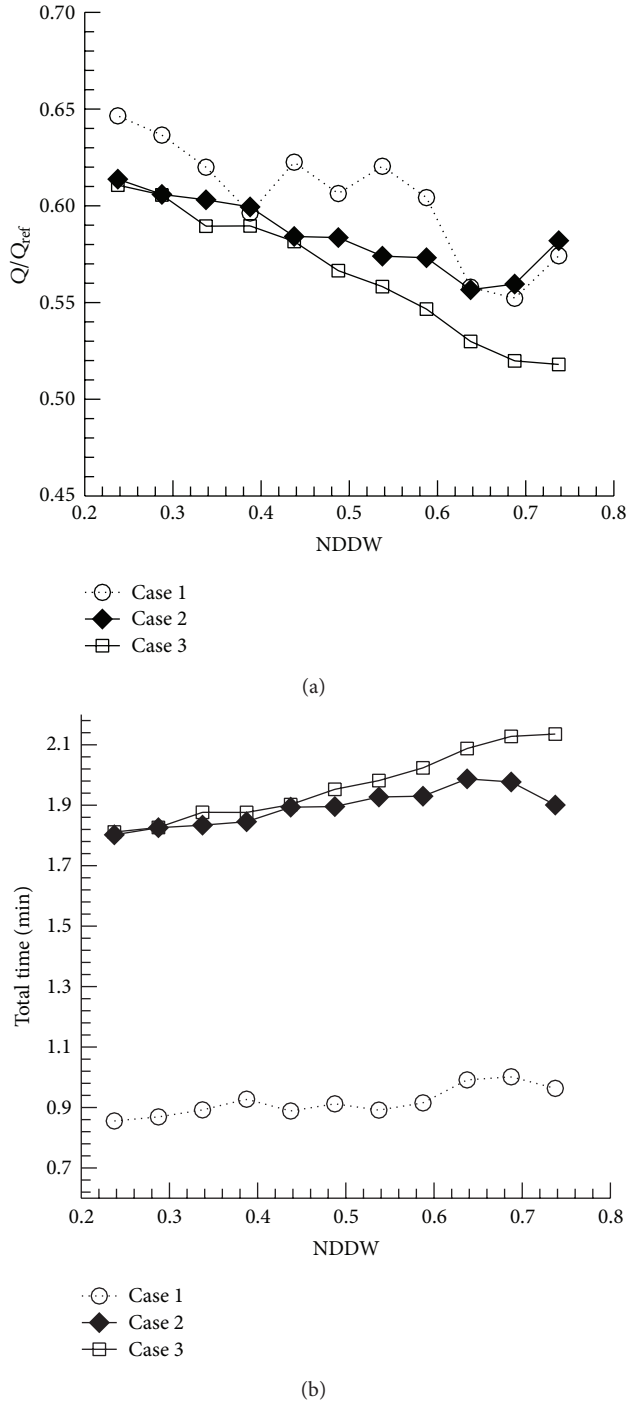

Figure 10: At different window locations (a) volumetric flow rate, (b) required time.

be one of the promising cross ventilation designs as long as the mixing level of the entered air is concerned. It can be easily found in most face to face cross ventilation systems that a large part of the entered air just passes the indoor distance (from inlet to outlet) directly without mixing with the interior air. Therefore, the natural cross ventilation system with diagonal window arrangement can be regarded as the

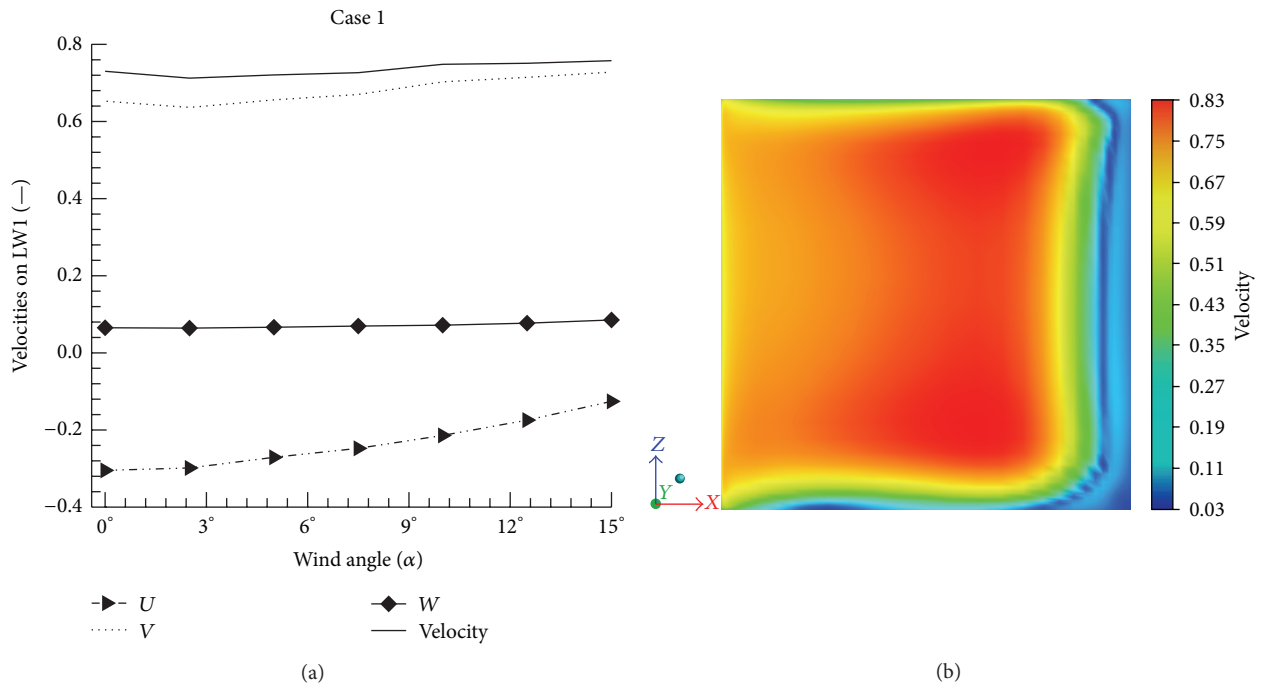

FIGURE 11: (a) Velocities on LW1 at different wind angles, (b) velocity contour on XZ plane in window 1.

effective ventilation system although it provides relatively lower ventilation rate (below 11%).

During designing a wind-driven naturally ventilated (cross) building, it is expected to design the orientation of the building in such a way that the wind direction is mostly parallel (i.e., $\alpha = 0^{\circ}$) to the length of the building so that the air can enter the building directly through the inlet window. But in a specific season, the local ambient wind direction around the building may change continuously in a moderate range due to the local temperature variation, landscape, the presence of static or moving objects, and so forth. From this point of view, it is necessary to analyze the sensitivity of the ambient wind direction on the ventilation system. To capture a larger wind angle effect (α) on the ventilation system, a sufficiently big computational domain is required to ensure the uniform approaching wind on the building and obviously it needs more computational cost and facility which is beyond the present arrangement. However, the present computational domain is sufficient enough to capture the effect of the wind angle in a range of 0°–15°. Furthermore, the larger wind angle is an off design situation and it is assumed that the wind angle does not change very much from that of the actual design ($\alpha = 0^{\circ}$).

In the present study, the wind angle (α) is varied keeping the free stream velocity ($U_R = 1.5$ m/s) constant and the windows are located at DWC = 1.475 m in Case 1 and Case 3. In Case 2, the windows are located at the mid of the corresponding wall (i.e., DWC = 0). As α increases, the approaching wind's U-component ($U_R \sin\alpha$) increases and V-component ($U_R \cos\alpha$) decreases. Therefore, it is reasonable that the velocity component W may not change with the change of α in the region where the approaching wind dominates the flow field. It is found that if a large wind angle effect is required to be analyzed, a sufficiently large computational domain around the building should be considered. Figure 11(a) presents the velocity distribution on line LW1 at different wind angle in Case 1. The magnitude of the velocity component U on LW1 decreases because this local U (negative) acts opposite to the approaching U. As the approaching U strengthens with the increase of α, the magnitude of the local U on LW1 weakens (Figure 11(a)). The sensitivity of α on the velocity at LW1 is examined in all cases. It shows decreasing-increasing trend with the increase of α in Cases 1 and 2, whereas it decreases in Case 3. One point should be noted here that the window wall has a thickness of 0.25 m and LW1–LW4 are located vertically at the mid of the thick windows (Figure 2). Therefore, the velocity on LW1 is a local phenomenon which may not reflect the ventilation rate as a whole. In Case 1 when $\alpha = 0^{\circ}$, the nondimensional velocity contour on a plane located in window 1 is depicted in Figure 11(b).

The wind pressure difference around the building's wall induces the cross ventilation through the windows. The pressure on the wall is subjected to wind speed and wind angle. The dependence of surface pressure coefficient ($C_p = (p - p_0)/0.5\rho U_0^2$) on the wind angle is shown in Figure 12. As we see, C_p of front wall, roof and the rear wall are reasonably invariant at $\alpha \in [0, 15^{\circ}]$. As α is increased, the pressure on the left wall is increased (Figure 12) due to the fact that more fluid particles act on the left wall. Similarly, the reverse phenomenon is observed on the right wall. It can be noted from the comparisons of Figures 12(a), 12(b), and 12(c) that

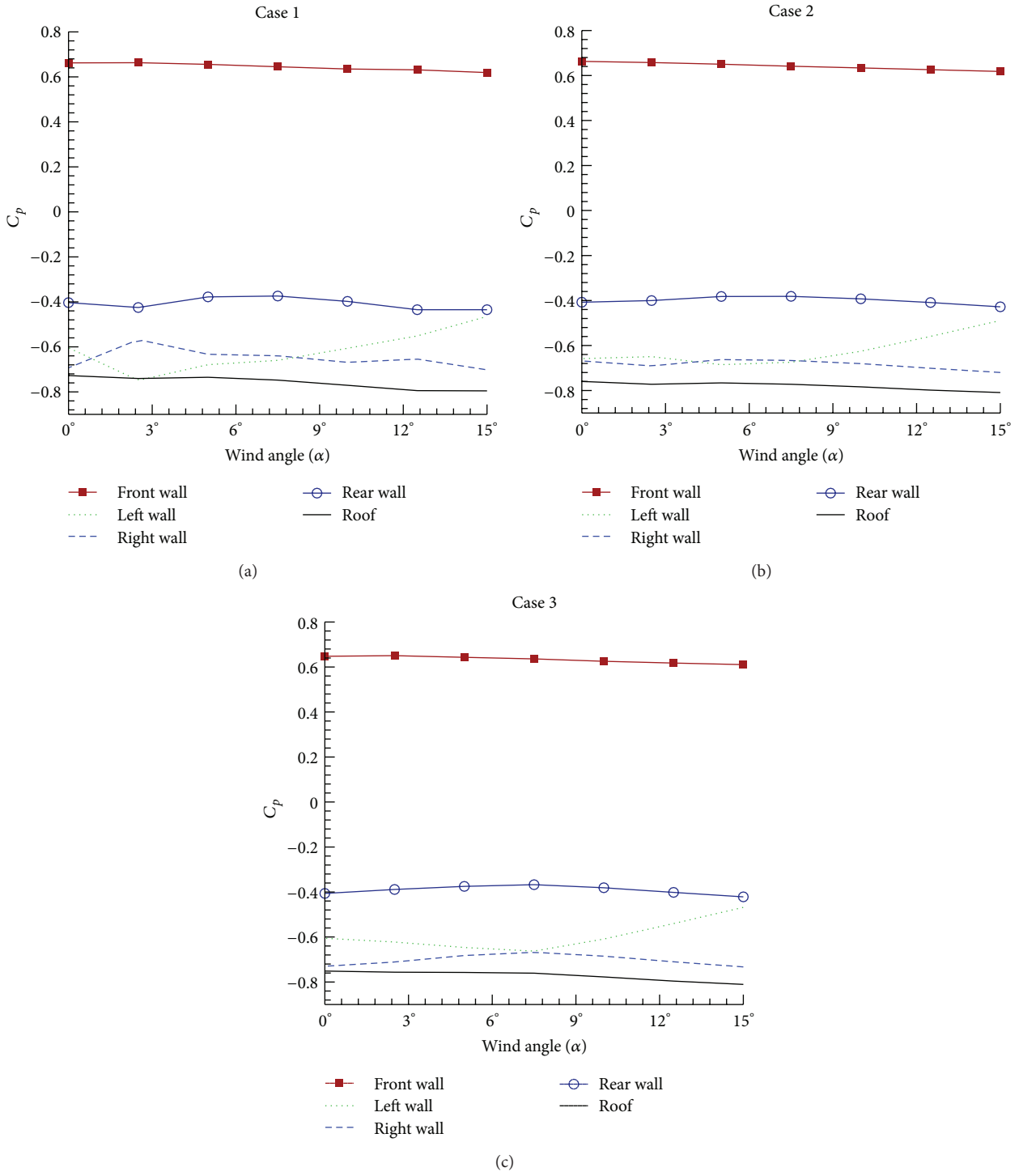

Figure 12: Average surface pressure coefficient at different wind angles.

the average C_p on different wall is also subjected to the position and the number of windows.

A few experimental/computational researches were reported where the wind angle was varied to analyze the sensitivity of the wind direction on the corresponding ventilation systems. Most cases had face to face opening (as in Case 2) to study the WDN cross ventilation systems. To the authors' knowledge, no case has been reported where cross ventilation with multiple windows (Case 1) and diagonally positioned windows (Case 3) were investigated and compared under the view of the wind angle (α) change. In the present study, the effects of the wind angle ($\alpha \leq 15^{\circ}$) on all cases have been investigated and compared as well. At nonzero wind angle, the ventilation through the two

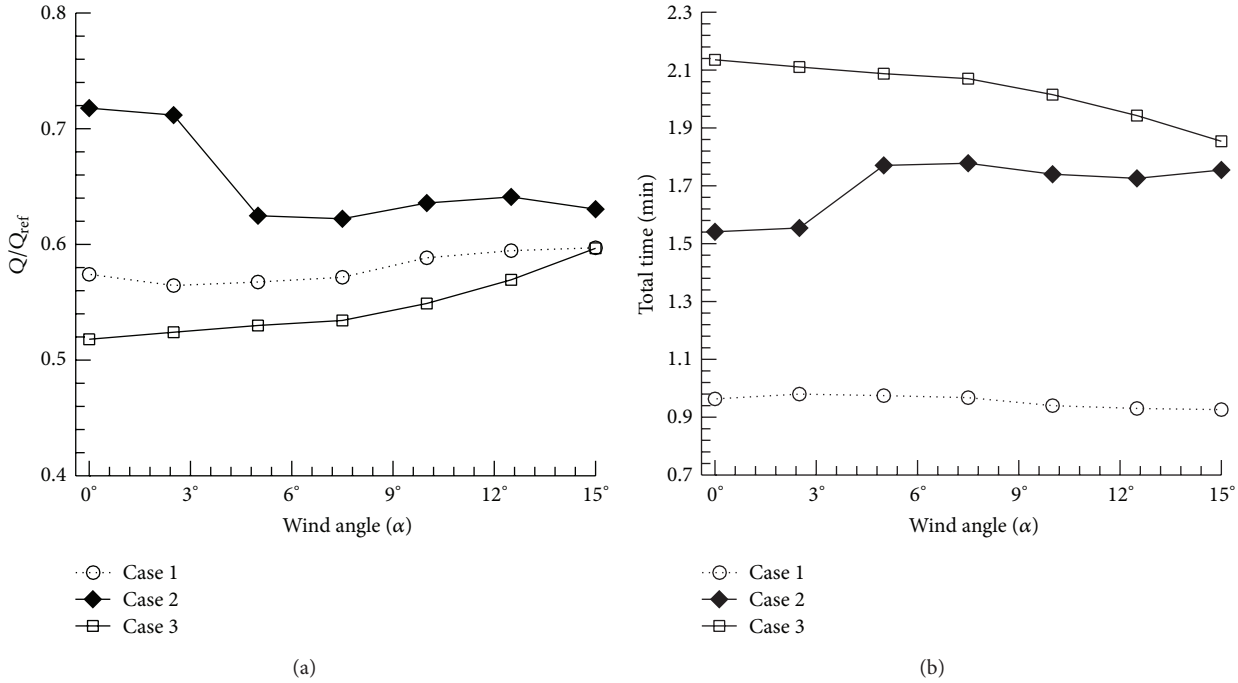

Figure 13: At different wind angles (a) volumetric flow rate, (b) required time.

front windows in Case 1 is not symmetric with respect to the indoor geometry and the flow direction. It is reasonably found that when α is increased, the flow through window 1 is increased, whereas it is decreased through window 2. When DWC = 1.475 m, the connecting straight line of window 1 and window 3 makes an angle 36.4° with the downstream direction (Y-axis). Therefore, if α is increased to 36.4° the part of air entering the building through window 1 may travel the indoor distance directly from window 1 to window 3. On the other hand, if $\alpha > 10.6°$, the entered air through window 1 may not directly pass the upright distance from window 1 to window 4 (Figure 2). Therefore, if the wind angle is changed in a specific range, the mixing level of the air may be increased that is one of main purposes of the ventilation system.

The ventilation rate is increased (and thus t is decreased) with the increment of α although the increasing rate is not exactly the same in Cases 1 and 3. The ventilation rate and the total time at different α are shown in Figure 13 for all cases. In Case 2, any introduction of wind angle ($\alpha > 0°$) will divert the fluid from direct passing from inlet to outlet that reduces the flow rate. From a simple calculation it can be stated that the amount of fluid that passes the indoor distance directly is reduced half at $\alpha = 5.3°$. The ventilation rate in Case 2 is the most sensitive to α among all cases in the range of $\alpha = 0°$–$6°$ and it is decreased up to 14% (at $\alpha = 5°$-$6°$) from the basic design ($\alpha = 0°$), whereas Q is increased up to 4% in Case 1 and up to 15% in Case 3. Therefore, it can be stated that if the wind angle is changed in a moderate range from its original design in Cases 1 and 3, the ventilation rate and the mixing quality is not reduced anyway rather it is increased and thus the ventilation purpose is served successfully. However, the ventilation rate may be reduced utmost 15% in Case 2 when $\alpha \in [0, 15°]$.

5. Conclusions

Three different cases of WDN cross ventilation systems were studied with the help of computational fluid dynamics (CFD). Using the valid methodology, a series of computations were carried out to predict and compare the ventilation performance in each case. The position of windows and the direction of wind were varied to investigate the effect of openings' lateral locations and wind direction on the performance of the present ventilation system. Comparing Case 1 with Cases 2 and 3, it can be reconfirmed that the ventilation rate is increased and thus the total time is decreased if the number of windows are increased. In Case 1, the windows located in the central area of the front wall may ventilate the air faster. However, if the windows are located far from each other it may ensure uniform mixing of the entered air with the indoor air. The effects of window locations in Case 2 can be concluded as follows: if the windows are located at the mid wall as well as in the corner area, the ventilation can be performed faster. In Case 3, the more the windows are close to each other, the higher the ventilation rate and thus the shorter the ventilation time are. In WDN cross ventilation, the length of the building is designed parallel to the wind direction so that the air packet can enter the building smoothly through the inlet. As the wind angle may change in off design situation, the sensitivity of the wind direction in a range of 0°–15° on the present WDN ventilation system is investigated. It is found that the average C_p on different wall is not only subjected to wind

angle but also subjected to the position and the number of windows. When the wind angle is changed in a moderate range from its original design, the ventilation rate is not reduced anyway rather it is increased in Case 1 and Case 3, and thus the design target of ventilation rates are surpassed. Although the ventilation rate may be reduced utmost 15% in Case 2 when $\alpha \in [0, 15^\circ]$, it may enhance the availability of uniform quality air at every section inside the building. In the present investigation, no temperature difference between the internal and the external air is considered which may not reflect the actual natural condition. A further study considering the buoyancy effect is expected to be carried out in future.

Nomenclature

A: Area of a window [m^2]
C_d: Discharge coefficient [—]
C_p: Mean pressure coefficient [—]
C_μ: k-ε turbulence model constant [—]
$C_{\varepsilon 1\mathrm{RNG}}$: RNG k-ε turbulence model coefficient
$C_{\varepsilon 2\mathrm{RNG}}$: RNG k-ε turbulence model constant [—]
$C_{\mu\mathrm{RNG}}$: RNG k-ε turbulence model constant [—]
H: Height of the building [m]
I: Turbulence intensity [—]
k: Turbulence kinetic energy per unit mass [$m^2 s^{-2}$]
L: Dimension of flat plate [m]
L_b: Dimension of the building [m]
L_w: Dimension of the window [m]
$\dot{m}$: Mass flow rate [$kg\, s^{-1}$]
p: Pressure [$kg\, m^{-1} s^{-2}$]
p_0: Free stream static pressure [$kg\, m^{-1} s^{-2}$]
Δp: Pressure difference [$kg\, m^{-1} s^{-2}$]
P_k: Shear production of turbulence [$kg\, m^{-1} s^{-3}$]
Q: Ventilation rate [$m^3 s^{-1}$]
Q_{ref}: Reference flow rate [$m^3 s^{-1}$]
Re_b: Reynolds number around a bluff body [—], $\mathrm{Re}_b = \rho H U_b/\mu$
Re_w: Reynolds number at an opening [—], $\mathrm{Re}_w = \rho L_w U_w/\mu$
t: Required time to replace the total internal air [minute]
U, V, W: x, y, and z-component of the velocity, respectively [$m\, s^{-1}$]
U_b: Velocity at the building [$m\, s^{-1}$]
U_R: Free stream velocity [$m\, s^{-1}$]
U_w: Velocity at a window [$m\, s^{-1}$]
v: Velocity [$m\, s^{-1}$]
v^*: Atmospheric boundary layer friction velocity [$m\, s^{-1}$]
v_h: Reference velocity at building height [$m\, s^{-1}$]
x, y, z: Cartesian coordinates [m]
z_0: Aerodynamic roughness length [m].

Greek Symbol

ρ: Density of the fluid [$kg\, m^{-3}$]
μ: Viscosity [$kgm^{-1} s^{-1}$]
ε: Turbulence dissipation rate [$m^{-2} s^{-3}$]
$\sigma_{k\mathrm{RNG}}$: RNG k-ε turbulence model constant [—]
$\sigma_{\varepsilon\mathrm{RNG}}$: RNG k-ε turbulence model constant [—].

Conflict of Interests

The authors declare that there is no conflict of interests regarding the publication of this paper.

Acknowledgments

The authors wish to appreciate the supports provided by the Department of Mathematics, University of Dhaka, Bangladesh, and by the Department of Aeronautics and Astronautics, National Cheng Kung University, Taiwan.

References

[1] H. B. Awbi, *Ventilation of Buildings*, Spon Press, London, UK, 2nd edition, 2003.

[2] M. Fordham, "Natural ventilation," *Renewable Energy*, vol. 19, no. 1-2, pp. 17–37, 2000.

[3] J. P. Cockroft and P. Robertson, "Ventilation of an enclosure through a single opening," *Building and Environment*, vol. 11, no. 1, pp. 29–35, 1976.

[4] J. E. Cermak, M. Poreh, J. A. Peterka, and S. S. Ayad, "Wind tunnel investigations of natural ventilation," *Journal of Transportation Engineering*, vol. 110, no. 1, pp. 67–79, 1984.

[5] P. Karava, T. Stathopoulos, and A. K. Athienitis, "Airflow assessment in cross-ventilated buildings with operable façade elements," *Building and Environment*, vol. 46, no. 1, pp. 266–279, 2011.

[6] E. Dascalaki, M. Santamouris, A. Argiriou et al., "Predicting single sided natural ventilation rates in buildings," *Solar Energy*, vol. 55, no. 5, pp. 327–341, 1995.

[7] R. Aynsley, "Estimating summer wind driven natural ventilation potential for indoor thermal comfort," *Journal of Wind Engineering and Industrial Aerodynamics*, vol. 83, pp. 515–525, 1999.

[8] Y. Li, "Buoyancy-driven natural ventilation in a thermally stratified one-zone building," *Building and Environment*, vol. 35, no. 3, pp. 207–214, 2000.

[9] T. S. Larsen and P. Heiselberg, "Single-sided natural ventilation driven by wind pressure and temperature difference," *Energy and Buildings*, vol. 40, no. 6, pp. 1031–1040, 2008.

[10] P. S. Carey and D. W. Etheridge, "Direct wind tunnel modelling of natural ventilation for design purposes," *Building Services Engineering Research and Technology*, vol. 20, no. 3, pp. 131–142, 1999.

[11] S. S. Ayad, "Computational study of natural ventilation," *Journal of Wind Engineering and Industrial Aerodynamics*, vol. 82, no. 1, pp. 49–68, 1999.

[12] Y. Jiang, D. Alexander, H. Jenkins, R. Arthur, and Q. Chen, "Natural ventilation in buildings: measurement in a wind tunnel and numerical simulation with large-eddy simulation," *Journal*

of Wind Engineering and Industrial Aerodynamics, vol. 91, no. 3, pp. 331–353, 2003.

[13] G. Evola and V. Popov, "Computational analysis of wind driven natural ventilation in buildings," *Energy and Buildings*, vol. 38, no. 5, pp. 491–501, 2006.

[14] B. Blocken, T. Stathopoulos, J. Carmeliet, and J. L. M. Hensen, "Application of computational fluid dynamics in building performance simulation for the outdoor environment: an overview," *Journal of Building Performance Simulation*, vol. 4, no. 2, pp. 157–184, 2011.

[15] K. S. Nikas, N. Nikolopoulos, and A. Nikolopoulos, "Numerical study of a naturally cross-ventilated building," *Energy and Buildings*, vol. 42, no. 4, pp. 422–434, 2010.

[16] M. Z. I. Bangalee, S. Y. Lin, and J. J. Miau, "Wind driven natural ventilation through multiple windows of a building: a computational approach," *Energy and Buildings*, vol. 45, pp. 317–325, 2012.

[17] M. Caciolo, P. Stabat, and D. Marchio, "Numerical simulation of single-sided ventilation using RANS and LES and comparison with full-scale experiments," *Building and Environment*, vol. 50, pp. 202–213, 2012.

[18] R. Ramponi and B. Blocken, "CFD simulation of cross-ventilation for a generic isolated building: impact of computational parameters," *Building and Environment*, vol. 53, pp. 34–48, 2012.

[19] J. Franke, C. Hirsch, A. G. Jensen et al., "Recommendations on the use of CFD in wind engineering," in *Proceedings of the International Conference Urban Wind Engineering and Building Aerodynamics*, von Karman Institute, Sint-Genesius-Rode, Belgium, 2004.

[20] V. Yakhot and S. A. Orszag, "Renormalization-group analysis of turbulence," *Physical Review Letters*, vol. 57, no. 14, pp. 1722–1724, 1986.

[21] ANSYS 12.0, Ansys, http://www.ansys.com/.

[22] F. M. White, *Viscous Fluid Flow*, McGraw-Hill, New York, NY, USA, 3rd edition, 2006.

[23] D. M. Hargreaves and N. G. Wright, "On the use of the k-ε model in commercial CFD software to model the neutral atmospheric boundary layer," *Journal of Wind Engineering and Industrial Aerodynamics*, vol. 95, no. 5, pp. 355–369, 2007.

[24] Y. Tominaga, A. Mochida, R. Yoshie et al., "AIJ guidelines for practical applications of CFD to pedestrian wind environment around buildings," *Journal of Wind Engineering and Industrial Aerodynamics*, vol. 96, no. 10-11, pp. 1749–1761, 2008.

[25] J. Smagorinsky, "General circulation experiments with the primitive equations, I. The basic experiment," *Monthly Weather Review*, vol. 91, no. 3, pp. 99–164, 1963.

[26] Q. Chen, "Comparison of different k-ε models for indoor air flow computations," *Numerical Heat Transfer B*, vol. 28, no. 3, pp. 353–369, 1995.

[27] P. Karava, *Airflow prediction in buildings for natural ventilation design: wind tunnel measurements and simulation [Ph.D. thesis]*, Concordia University, Quebec, Canada, 2008.

[28] P. J. Richards and R. P. Hoxey, "Appropriate boundary conditions for computational wind engineering models using the k-ϵ turbulence model," *Journal of Wind Engineering and Industrial Aerodynamics*, vol. 46-47, pp. 145–153, 1993.